The Origin of Band Structure

Contents

Abstract

Characteristic for much of the electronic behavior in solids is the existence of energy bands, separated by bandgaps. The bands are permitted for occupation with carriers, and their origin can be described by two complementary models. The *proximity approach* considers the effect of the neighborhood in a solid on the energy levels of an isolated atom; this model is particularly suited for organic semiconductors, amorphous semiconductors, and clusters of atoms. The *periodicity approach* emphasizes the long-range periodicity of the potential in a crystal. Electrons near the lower edge of a band in a crystal behave akin to electrons in vacuum; the influence of the crystal potential is expressed by an *effective* electron mass which increases with increasing distance from the band edge. This chapter describes the basic elements of the electronic band structure in solids.

Keywords

Band structure · Bandgap · Bloch function · Effective mass · HOMO · Kronig-Penney model · LUMO · Organic crystals · Periodicity approach · Proximity approach · Reduced k vector

K.W. Böer, U.W. Pohl, *Semiconductor Physics*,
https://doi.org/10.1007/978-3-319-69150-3_6

1 Approaches for Modeling

Electronic transitions in energy and in space are the basic processes of interest in semiconductor physics. The first group is responsible for the large variety of excitation and de-excitation (recombination) processes; the second must be considered for carrier transport. Both are characterized by quantum-mechanical features: the spectrum of electronic energy states (*eigenstates*), the distribution of electrons over these states, and the interactions that cause changes in this distribution.

The general principles that yield the spectrum of energy states typical for the solid semiconductor are discussed first. The main features of this spectrum are obtained using two apparently different models, which both are applied to describe crystals. The first model, referred to as the *proximity approach*, starts from individual atoms and its immediate neighborhood and expands with less and less attention to the atomistic structure the further one extends from the origin. This approach is also successfully used for amorphous semiconductors. The second model, the *periodicity approach*, is at first view rather insensitive to the detailed properties of individual atoms but considers the long-range periodicity of a crystalline lattice. Both yield similar qualitative results: spectra of broad, permitted ranges of energy which, in space, extend as *bands* throughout the entire semiconductor and which are interspersed with forbidden ranges.

In this chapter both the proximity and the periodicity approach are presented, and common features along with some of the differences in the results are pointed out. The discussion starts from a rather heuristic description and introduces sequentially more sophisticated elements.

1.1 The Proximity Approach

In a simple first step, the exchange of electrons between two atoms can be made plausible by considering the splitting of eigenstates of degenerate oscillators, i.e., oscillator states having the same eigenfrequency, when they become coupled with each other. This splitting increases as the coupling gets stronger, corresponding to a closer approach of two atoms. The addition of more atoms of the same kind at increased distances splits the energy levels into more levels which span a *range* of energies. If the levels are spaced closely enough, *Heisenberg's uncertainty principle* no longer permits distinction between the individual levels.[1] In this case, one obtains

[1]Applying $\Delta E \Delta t \cong \hbar$ and relating Δt to the time an electron resides at a sufficiently high energy level E_{ik} (later identified as belonging to an upper band), an uncertainty of ΔE results. The time Δt is related to scattering (see ▶ Sect. 2 in chapter "Carrier-Transport Equations"); the electron is removed from this level after $\lambda/v_{\mathrm{rms}} \approx 10^{-12}$ s, yielding an uncertainty of ~1 meV, which is on the same order as the splitting provided by only 10^4 atoms (assuming a band width of ~1 eV and an equidistant splitting of 1 level per added atom – that is, within a crystallite of <100 Å diameter. With larger crystallites the splitting is even closer and results in a level continuum.

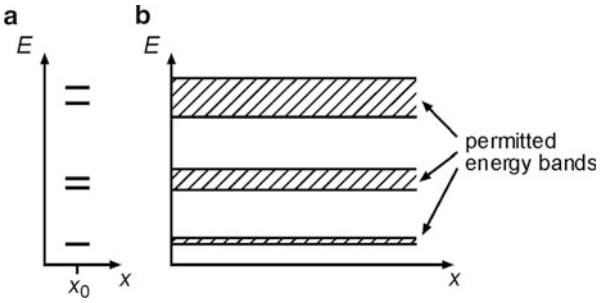

Fig. 1 (**a**) Splitting of eigenstates when two atoms have approached each other. (**b**) Simple band model of a crystal consisting of many atoms

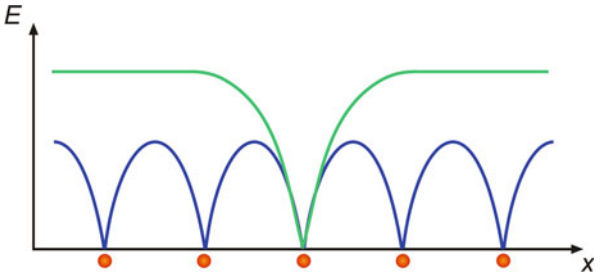

Fig. 2 Potential energy of an electron in an atom (*green curve*) and of an electron in an atomic cluster (*blue curve*); *red dots* below the abscissa indicate positions of atom cores

an *allowed energy range* in a sufficiently large cluster of atoms, instead of a discrete energy-level spectrum of a single atom or an aggregate of a few atoms – see Fig. 5. Since outer shell electrons can be exchanged more easily, the energy ranges created from valence electrons will be wider than the ranges created from the shielded inner electrons. The latter will more closely resemble the discrete eigenstates of isolated atoms. Since the same atoms behave alike, this allowed energy range extends throughout the crystal. In two dimensions (x,E) one therefore can draw allowed *energy bands* separated by *forbidden gaps* (Fig. 1).

In Fig. 1 the total electron energy is drawn disregarding the potential energy that an electron experiences when separated from an individual atom, which is shown in Fig. 2 for a single atom (upper curve, in green) and for a small one-dimensional cluster (blue curve). The band model emphasizes the *collective behavior*, i.e., the *sharing* of the electron among the atoms of the cluster. The potential distribution picture, on the other hand, emphasizes the *localization* of an electron within each potential funnel. Both pictures are valid: the band picture is more relevant for higher bands, while the potential picture is more relevant for lower (core) levels.

When the band picture is superimposed to the picture of the individual potentials of many adjacent atoms (Fig. 3), we recognize that the semiclassical approach, in which electrons may only move above potential barriers, is inappropriate, since bands indicate that electronic exchange exists well below the crest of the barriers. The origin of the electron transfer through such barriers is *tunneling*, i.e., a *quantum-mechanical* exchange, – see ▶ Sect. 2.3 in chapter "Carrier Generation."

This heuristic approach will now be expanded to motivate the formation of bands in a more appropriate quantum-mechanical analysis. The analysis is first applied to a

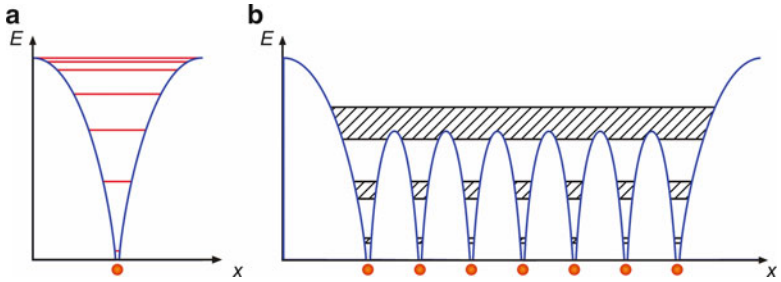

Fig. 3 Potential energy and eigenstates of electrons in (**a**) an atom and (**b**) a small crystal

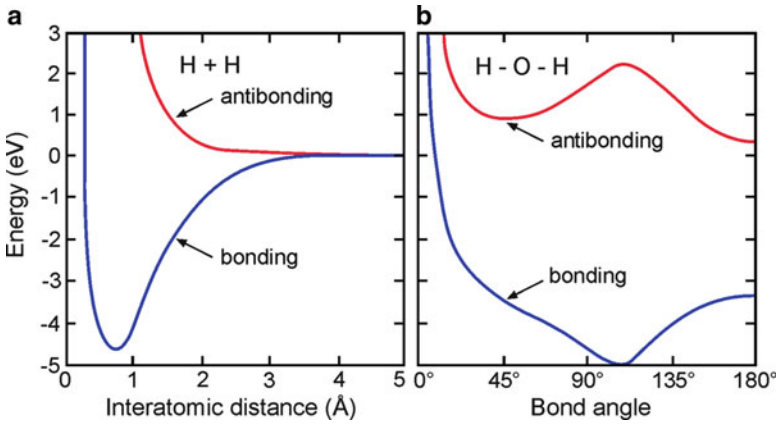

Fig. 4 Electron energy as a function of (**a**) the interatomic distance of a hydrogen molecule and (**b**) the bond angle in H_2O

cluster of atoms that forms the building block of an amorphous semiconductor and then to a periodic lattice.

1.1.1 Electronic Structure of Amorphous Semiconductors

The electron energy depends sensitively on the interatomic distance and bond angle, as shown for a simple H_2 and an H_2O molecule in Fig. 4. The bonding and antibonding curves reflect antiparallel and parallel spin of the electrons in the bonds, respectively.

The electronic structure of an amorphous or crystalline solid can be obtained by starting from an arbitrary atom and including more and more neighbors in an appropriate configuration; the eigenfunctions of such a cluster are determined by solving its Schrödinger equation. This is referred to as a *tight-binding approach*. Solutions can be obtained numerically, using reasonable approximations (Reitz 1955; Heine 1980; Slater and Johnson 1972; Kaplan and Mahanti 1995 – see also

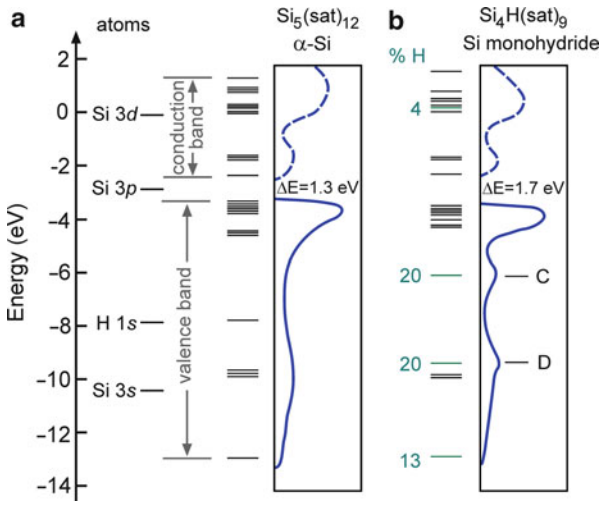

Fig. 5 Electron energy-level distribution for bonding (valence band) and antibonding (conduction band) states of a 17-atom cluster and optical density of states (see ▶ Sect. 1 in chapter "Band-to-Band Transitions") for (**a**) α-Si and (**b**) α-Si:H. Amorphous silicon α-Si is modeled by a Si-$(SiH_3)_4$ cluster denoted $Si_5(sat)_{12}$ with a central Si bond to 4 Si, each of which is saturated by 3 H. In the hydrogenated cluster 1 H atom is substituted for 1 Si, yielding a SiH-$(SiH_3)_3$ cluster corresponding to a Si:16% H alloy. Principal hydrogen-induced levels are marked in green and labeled according to the H contribution in the molecular orbitals (After Johnson et al. 1980). The agreement with the experimental bandgap of such a small cluster is spurious, however, and should not be over-evaluated. The calculated bandgap depends substantially on the boundary conditions

chapter ▶ "Quantum Mechanics of Electrons in Crystals"). The analysis can be described as that for a large molecule of, say, 20–50 atoms and delivers a spectrum of *energy eigenvalues* that, when the cluster is large enough, presents a valuable estimate of the energy bands of the solid.

Several Si atoms which form such a cluster produce the typical sp_3 bonding and antibonding states that are generated when the atoms are close enough – see ▶ Sect. 1.2 and ▶ Fig. 6 in chapter "Crystal Bonding." For a small cluster of Si atoms in an "amorphous configuration" (▶ Sect. 3.2 in chapter "The Structure of Semiconductors"), we calculate an eigenvalue spectrum (Fig. 5a) and see that the proximity to other Si atoms significantly changes and splits the atomic levels (shown on the left). They are split by a large amount and are distributed unevenly in energy. A much larger number of atoms, however, are required to create a truly band-like level distribution. The spectrum changes significantly when hydrogen is added to this cluster, which forms a bridging hydrogen structure (Ovshinsky and Adler 1978). It removes states from the gap of α-Si and thereby increases the bandgap from 1.3 eV for α-Si to 1.7 eV for the technically more interesting, hydrogenated α-Si:H (Eberhart et al. 1982; Street 2005).

When more atoms of the same kind are incorporated within such a cluster, more levels appear *within* the two bands, i.e., within the range of bonding and

antibonding states. These bands have been labeled in Fig. 5 as the conduction and valence bands; for more detailed definitions, see ▶ Sect. 1 in chapter "Bands and Bandgaps in Solids." The finite-cluster approach always overestimates the bandgap energy, since, by necessity, this approach omits states present which are far away from the center in **k** space and in direct bandgap materials (▶ Sect. 2 in chapter "Band-to-Band Transitions") lie near the edges of the bandgap.

From these examples, we can deduce that some information about the energy width of the upper energy bands and the bandgap can be obtained from clusters containing only ~50 atoms in an appropriate structural configuration. That is, the outer atoms must be kept artificially at positions they would attain when interacting with the surrounding atoms within a much larger amorphous network of atoms. The level distribution *within* a band, however, is poorly represented by such small clusters. The incorporation of many more atoms presents major computational problems for amorphous semiconductors; however, this problem becomes exceedingly simple in the periodic lattice of a crystalline semiconductor. For more reading, see Adler (1985), Agarwal (1995), Beeby and Hayes (1989), Shinozuka (1999), and Singh and Shimakawa (2003).

1.2 The Periodicity Approach

The behavior of electrons in a semiconductor can be approximated by assuming that they are nearly *free electrons* but interact with the *periodic potential* that simulates the lattice. In order to distinguish the influence of this periodic potential, one should first recall the behavior of a free electron with mass m_0*in vacuum*. This is determined by the solution of the *Schrödinger equation*

$$\frac{\partial^2}{\partial \mathbf{r}^2}\psi + \frac{2m_0}{\hbar^2}E\psi = 0, \tag{1}$$

which can be described by an *electron wave*

$$\psi(\mathbf{r}) = A\exp(\pm i\,\mathbf{k}\cdot\mathbf{r}), \tag{2}$$

with A as an amplitude factor. The *wavevector* **k** relates to electron momentum and energy as

$$\mathbf{k} = \frac{m_0\mathbf{v}}{\hbar} = \frac{\mathbf{p}}{\hbar}, \qquad E = \frac{m_0}{2}v^2 = \frac{p^2}{2m_0} = \frac{\hbar^2k^2}{2m_0}, \tag{3}$$

or, more accurately, to the expectation value of the momentum given by

$$\langle\mathbf{p}\rangle = \int_{-\infty}^{\infty}\psi^*\frac{\hbar}{i}\frac{\partial}{\partial\mathbf{r}}\psi\;\,d\mathbf{r} = \hbar\mathbf{k}\int_{-\infty}^{\infty}\psi^*\psi = \hbar\mathbf{k}. \tag{4}$$

The wavevector **k** is the reduced wavevector – see the discussion later in this section and Fig. 13. Hence, $E(\mathbf{p})$ or $E(\mathbf{k})$ is described by a three-dimensional paraboloid

(by a parabola in one relevant coordinate) with one electronic parameter, the *electron rest mass* m_0.

Equation 2 represents an electron wave with a wavelength, the *de Broglie wavelength*,[2] of

$$\lambda_{\mathrm{DB}} = \frac{2\pi}{k} = \frac{h}{|p|} = \frac{h}{m_0 v} = \frac{7.27}{v\ (\mathrm{cm/s})}\ \ (\mathrm{cm}) \tag{5}$$

or, when introducing the electron energy from Eq. 3,

$$\lambda_{\mathrm{DB}} = \frac{h}{\sqrt{2m_0 E}} = \frac{12.26}{\sqrt{E(\mathrm{eV})}}\,(\mathrm{Å}). \tag{6}$$

An electron in the lattice, i.e., when it is exposed to a periodic potential, no longer behaves like a free particle: it experiences interference from the lattice potential when, with increasing electron energy, its de Broglie wavelength becomes comparable to the lattice constant. The ensuing *Bragg reflections* prohibit a further acceleration of the electron, described later in more detail. This simple discussion also indicates the existence of a finite energy range, the energy band in a semiconductor. Near the bottom band edges, the electron behaves to some extent like a free electron, i.e., like a classical particle. The quantum-mechanical nature becomes evident when it gains energy in an electric field or is forced to occupy higher states. At energies of 4 eV, the de Broglie wavelength is 6 Å, i.e., small enough to permit interference effects within the periodic potential of the lattice. This plausibility argument can be substantiated by describing the electron with a wave equation, the Schrödinger equation, and by introducing into the Schrödinger equation a periodic potential $V(\mathbf{r})$,

$$\frac{\partial^2}{\partial \mathbf{r}^2}\psi + \frac{2m_0}{\hbar^2}\left(E(\mathbf{k}) - V(\mathbf{r})\right)\quad \psi = 0. \tag{7}$$

The solutions of this Schrödinger equation are so-called Bloch functions which can be expressed as a linear combination of waves

$$\psi_n(\mathbf{k},\mathbf{r}) = u_n(\mathbf{k},\mathbf{r})\exp(i\ \ \mathbf{k}\cdot\mathbf{r}), \tag{8}$$

with n as the band index specifying a certain band. The waves are plane waves with a space-dependent amplitude factor $u_{\mathrm{n}}(\mathbf{k},\mathbf{r})$, which shows lattice periodicity (Bloch's theorem, 1928; see ▶ Sect. 1.2 in chapter "Quantum Mechanics of Electrons in Crystals"). A one-dimensional schematic representation is given in Fig. 6 to indicate the relationship between the lattice potential $V(\mathbf{r})$ and the Bloch function $\psi_{\mathrm{n}}(\mathbf{k},\mathbf{r})$,

[2]The de Broglie wavelength is on the same order of magnitude as the uncertainty distance obtained from Heisenberg's uncertainty principle $\Delta x \geq \hbar/\Delta p_x$, which has the same form as λ_{DB}. This yields uncertainty distances of 10 Å for thermal (free) electrons at room temperature.

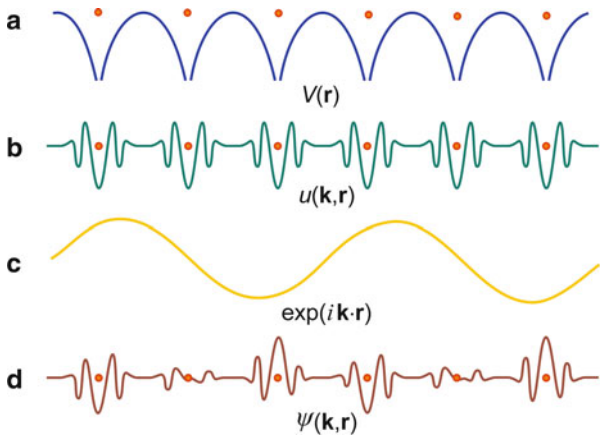

Fig. 6 A schematic representation of electronic eigenstates in a crystal. (**a**) The potential $V(\mathbf{r})$ plotted along a row of atoms; (**b**) $u(\mathbf{k},\mathbf{r})$, which has the periodicity of the lattice; (**c**) a plane electron wave, the real part of which is shown to construct the electron wavefunction; and (**d**) a Bloch function; the state itself is complex, and only the real part is shown. The Bloch function is composed of the product of (**b**) and (**c**)

which contains $u_n(\mathbf{k},\mathbf{r})$ and the plane wavefunction of the electron $\exp(i\mathbf{k}\cdot\mathbf{r})$, to construct the electron wavefunction (Harrison 1980a).

Inserting Eq. 8 into Eq. 7, we obtain the result that solutions exist only for certain ranges of the electron energy $E_n(\mathbf{k})$, which are interspersed with energy ranges in which real solutions do not exist. This confirms the previously obtained results that the energy spectrum in a solid consists of alternating allowed and forbidden energy ranges (energy bands). The periodic-potential approach, however, gives additional information that can be demonstrated readily in a simple one-dimensional model.

1.2.1 The Kronig-Penney Model

An enormously simplified periodic potential $V(x)$ is sufficient for introduction into Eq. 9 to show the typical behavior. This is the *Kronig-Penney potential* (Kronig and Penney 1931),[3] which is shown in Fig. 7. Since the discussion of this behavior is rather transparent, it will be used here for an introduction to the basic features of the band model.

Introducing Eq. 8 into Eq. 7 for one relevant dimension, we see that $u(x)$ must satisfy

[3]In one dimension, there are other periodic potentials for which the Schrödinger equation can be integrated explicitly. $V(x) = -V_0\,\mathrm{sech}^2(\gamma x)$ is one such potential, which yields solutions in terms of hypergeometric functions (see Mills and Montroll 1970). The results are quite similar to the Kronig-Penney potential.

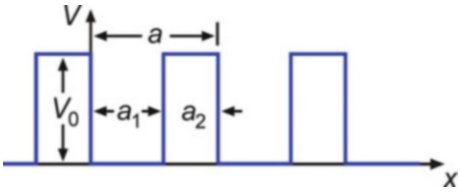

Fig. 7 Kronig-Penney potential with V_0 the barrier height, a_1 and a_2 the well and barrier widths, respectively

$$\frac{d^2u}{dx^2} + 2ik\frac{du}{dx} - \left(k^2 - \frac{2m_0[E - V(x)]}{\hbar^2}\right) \quad u = 0. \tag{9}$$

We can split Eq. 9 after the introduction of the Kronig-Penney potential into two differential equations: one for the bottom of the well and one for the top of the barrier with a potential $V = V_0$. The solutions in each part can be expressed as the sum of two waves:

$$\begin{aligned} u_1(x) &= A\exp[i(\alpha - k)x] + B\exp[-i(\alpha + k)x] \quad \text{for} \quad 0 < x < a_1 \\ u_2(x) &= C\exp[i(\beta - k)x] + D\exp[-i(\beta + k)x] \quad \text{for} \quad -a_2 < x < 0, \end{aligned} \tag{10}$$

where α and β are the k values for a free electron in vacuum, for $V = 0$, and for a constant barrier potential V_0, respectively:

$$\alpha = \sqrt{\frac{2m_0E}{\hbar^2}} \quad \text{and} \quad \beta = \sqrt{\frac{2m_0(V_0 - E)}{\hbar^2}}. \tag{11}$$

The integration constants can be determined by the continuity requirements of $u(x)$ and its first derivatives at $x = a_1$ and $x = a_2$, which yield[4]

$$-\frac{\alpha^2 - \beta^2}{2\alpha\beta}\sin(\alpha a_1)\sinh(\beta a_2) + \cos(\alpha a_1)\cosh(\beta a_2) = \cos(ka). \tag{12}$$

Equation 12 provides the *dispersion relation* $E(k)$ (E is contained in α and β).

The dispersion relation is the key to many discussions of electronic properties in solids. Since the wavenumber k is proportional to the electron momentum (Eq. 3), the dispersion equation relates the electron energy to mass and velocity, both of which are essential for understanding the specific behavior of electrons in a semiconductor. This will be explained in detail in several of the following sections.

[4]For $E > V_0$, the square root in β becomes imaginary. Introducing $\gamma = i\sqrt{2m_0(e - V_0)/\hbar^2}$ and with $\sinh(i\gamma) = i\sin\gamma$ and $\cosh(i\gamma) = i\cos\gamma$, we obtain for higher electron energies a similar equation:

$$-\frac{\gamma^2 + \alpha^2}{2\alpha\gamma}\sin(\gamma a_2)\sin(\alpha a_1) + \cos(\gamma a_2)\cos(\alpha a_1) = \cos(ka).$$

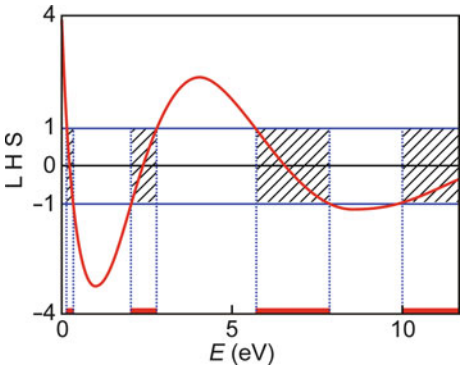

Fig. 8 Left-hand side (LHS) of Eq. 12 as a function of E (contained in α and β), computed for $a_1 = 6$ Å, $a_2 = 1.2$ Å, and $V_0 = 10$ eV

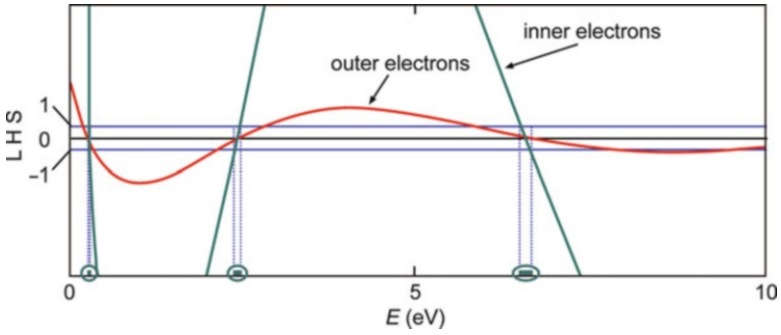

Fig. 9 LHS as in Fig. 8, but for two different values of the parameter V_0 (10 eV for curve labeled "outer electrons" and 40 eV for "inner electrons" – other parameters as in Fig. 8), indicating the reduced width of the permitted bands for higher potential barriers (i.e., for inner electrons that are more tightly bound) represented by encircled *green* bars at the E axis

Equation 12 reveals that a sequence of allowed energy ranges (*bands*) is interspersed with forbidden energy ranges: energy gaps are formed when the left-hand side (LHS) of Eq. 12 exceeds ± 1, which are the limiting values of the equation's right-hand side. In Fig. 8 the hatched ranges show the energy bands; no solution of the Schrödinger equation can be found between the bands for real values of k. This picture describes a situation between a free electron in vacuum, where *all energies* are permitted, and an electron bound to an isolated atom, where the permitted energy ranges shrink to a *set of discrete energy levels*. The height and width of the potential barriers and wells (a_1, a_2, and V_0) determine whether an electron behaves more like an electron bound to a single atom (large a_2/a_1 and V_0) or more like a free electron in vacuum (small a_2 and V_0); see Fig. 9. In the latter example the permitted ranges extend over a wider energy range.

More information can be deduced from the $E(k)$ behavior within each of the permitted energy ranges shown in Fig. 10. At the bottom of the first permitted energy range, $E(k)$ is nearly parabolic. Then E moves with increasing k through an inflection

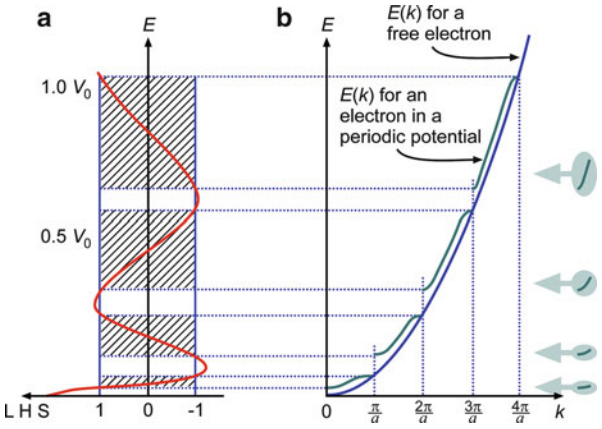

Fig. 10 (**a**) As Fig. 8, however, for a larger a_1/a_2 ratio. (**b**) $E(k)$ for a free electron (parabola) and for a Kronig-Penney potential in an extended wavenumber $E(k)$ representation. *Bottom* segments of the bands shown at the *right* indicate the increased curvature at the edge of higher bands

point and, at the top of this range, becomes nearly parabolic again but with a negative curvature.

Compared to the parabola of the free electron, the lower part of the $E(k)$ curve is raised. At the upper edge of the first allowed range, i.e., at $k = \pm\pi/a$, the curve coincides again with the free electron parabola. The next permitted band starts after a jump in E from E_1 to E_2 at $k = \pm\pi/a$ and has a similar $E(k)$ behavior as the first energy band, except that the curvatures are larger at the bottom and top of the band. The top is reached at $k = \pm 2\pi/a$, where again a jump of E occurs, from E_2 to E_3, etc. (Fig. 10). This behavior continues for higher bands with broader allowed bands, gradually increased curvature at the bottom and the top, and narrower bandgaps. Figure 10 also contains $E(k)$ for the free electron (Eq. 3), which is parabolic in the entire $E(k)$ range.

This general behavior is independent of the actual shape of the periodic potential as long as it has sufficient strength. Although periodicity of $V(x)$ is a necessary – but not sufficient – condition for energy bands with interspersed forbidden gaps, it so happens that in solids, for inner shell electrons, the potential barriers are sufficiently high to cause rather narrow, lower bands. Electrons at sufficiently high energies occupy wider bands and behave more like free electrons: they can move readily through the lattice. They will, however, be subject to interference with the periodic lattice potential (see Sect. 2.2).

When analyzing the effect of a *three-dimensional* periodic potential and using a real lattice potential, the actual $E(k)$ behavior becomes more complex; however, it still maintains the basic features of *energy bands* interspersed with *bandgaps*. This fundamental behavior is the basis for the electronic behavior of semiconductors and is described in more detail in many textbooks of solid state physics, e.g., Anderson (1963), Ashcroft and Mermin (1976), Bube (1992), Callaway (1976), Fletcher (1971), Harrison (1980b), Haug (1972), Kittel (2007), Marder (2010), and Ziman (1972).

1.3 Periodicity Versus Proximity Approach

The proximity of a sufficient number of atoms and the periodic lattice structure of a crystal both lead to allowed energy bands interspaced by bandgaps. We may use one or the other picture to obtain further information about the band structure.

The *periodic lattice-structure approach* is more suited for obtaining the specific $E(k)$ structure of the inner part of the band (near $k = 0$) which cannot be obtained from the proximity approach. It reflects the symmetry of the lattice and allows for obtaining the results in the most economical way. Its results, however, are restricted to periodic lattices, i.e., to crystals. This refers specifically to interference phenomena involving diffraction from further-than-nearest and next-nearest neighbor distances. These distances, however, can still be discerned in the x-ray diffraction of amorphous semiconductors and therefore may also be expected to influence electron behavior further away from $k = 0$.

The *proximity approach* can be used to obtain some information about the inside of the bands for first orientation. However, the inadvertent inclusion of artificial states at the surface of the cluster and the requirement for an extremely large cluster size to provide band states close to the band edges have been the handicaps of this approach.

A *supershell approach* is sometimes used to avoid some of the shortcomings of the periodic lattice and proximity approaches. This approach takes a cluster of sufficient size and repeats it *periodically* until the entire crystal volume is filled. In this way the mathematical methods developed for studying periodic lattices can be used, while certain elements of an amorphous structure are included in the cluster. The error due to the forced adjustment of each cluster can be minimized by increasing the size of the cluster.

Many of these results are important for understanding the behavior of metals (e.g., overlapping bands), but will not be discussed here. Other results relate to semiconductors, including semiconductor-metal transitions (see ▶ Sect. 3 in chapter "Equilibrium Statistics of Carriers"). Some heuristic examples of near-band-edge properties are given below.

1.3.1 Band-Edge Fluctuation

The ideal periodicity of a crystal lattice can be modified for a number of reasons, among them lattice oscillations or displaced lattice atoms. An amorphous semiconductor, for example, may be described by having frozen-in large fluctuations of the interatomic distances and bond angles. In some respects such structures are "almost crystalline," but with slightly changing lattice parameters, occurring particularly in the third-neighbor distance and beyond; see Fig. 29 in chapter ▶ "The Structure of Semiconductors". The good short-range order in an amorphous semiconductor leads to a band structure comparable to that of a perfectly ordered crystal; however, a lattice with a different lattice constant causes a different $E(\mathbf{k})$ with a different width of allowed bands and gaps. Therefore, we expect variations of the *band edges* in time

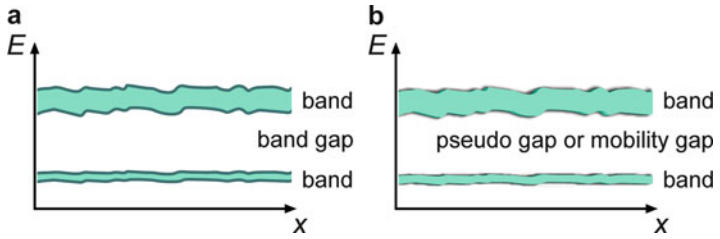

Fig. 11 (**a**) Perturbed and (**b**) fuzzed-out band edges in a crystal with phonons and in an amorphous semiconductor

and space.[5] Rather than being perfectly straight, the band edge becomes perturbed. Over a time average, and the band edge appears to be fuzzed out (Fig. 11). For further detail see chapter ▶ "Defects in Amorphous and Organic Semiconductors."

1.3.2 Discrete Defect Level in the Bandgap

When a local deviation from the ideal lattice structure is sufficiently large, the eigenstate of a *disordered atom* may lie within the bandgap. A plausibility argument may be obtained from the proximity model.

Assume an extra atom is incorporated in an *interstitial site* of the lattice (later discussed in ▶ Sect. 2.1 in chapter "Crystal Defects"). This extra atom is much closer to its neighbors; the exchange frequency is substantially larger than that for the nearest neighbors which yield the largest exchange frequency in an ideal lattice (equivalent to the band edges). Thus, the eigenstates of this interstitial atom, here an *intrinsic point defect*, and *its* nearest neighbors lie outside of the allowed bands of the ideal lattice, i.e., within the bandgaps (Fig. 12).

Energy states within the gap are *localized* at the position of this lattice defect (x_0 in Fig. 12) and play an important role in localizing (*trapping*) electrons in real crystals (see ▶ Sect. 2 in chapter "Deep-Level Centers") and in amorphous semiconductors. It also becomes reasonable to expect an energy distribution of such localized (*trap*) levels in the gap near the band edge, when taking into consideration that in crystalline and amorphous semiconductors a wide variety of lattice imperfections and lattice parameter variations are observed. In ▶ Sect. 3 of chapter "Optical Properties of Defects" and in chapter ▶ "Defects in Amorphous and Organic Semiconductors" we will return to this level distribution near the band edge.

[5]This concept must be used with caution, since **k** is a good quantum number only when electrons can move without scattering over at least several lattice distances. That is certainly not the case in most amorphous semiconductors near the "band edge" (see ▶ Sect. 4 in chapter "Carrier Transport Induced and Controlled by Defects"). However, at higher energies further inside the band, there is some evidence that the mean free path (▶ Sect. 2 in chapter "Carrier-Transport Equations") is much larger than the interatomic distance even in amorphous semiconductors. In bringing the two approaches together, the argument presented here lacks rigor and has plausibility only in terms of correspondence.

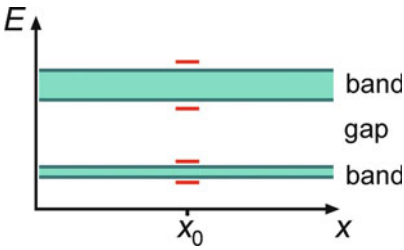

Fig. 12 Simple intrinsic atomic interstitial (i.e., an atom being chemically identical to the atoms of the crystal) in an idealized lattice

2 The Reduced k Vector

A general feature of the solutions of the Schrödinger equation is the periodicity of $E(k)$, illustrated in Fig. 13b. The figure shows the periodicity in $\mathbf{k}$ along k_x with a period length of $k_x a = 2\pi$. This means that a shift of the solution $E(k_x)$ by $2\pi/a$ in k_x represents the same behavior. Fig. 13a contains a copy of Fig. 10, indicating the relation to the periodicity of $E(k)$ shown in Fig. 13b. Any full segment of the periodic representation is a *reduced k-vector representation*. One such segment is shown within the first *Brillouin zone* in Fig. 13c, i.e., within $-\pi/a < k_x < \pi/a$. For a three-dimensional lattice, the reduced representation is discussed in ▶ Sect. 4 in chapter "Quantum Mechanics of Electrons in Crystals."

The reduced representation $E(k)$ shows an alternating sign of the curvature at the edge of each band at $k = 0$. It is positive for the first band, negative for the second, etc. This interesting peculiarity occurs in real crystals in a somewhat similar fashion, although is more complex because of a multiplicity of bands, as will be discussed in ▶ Sect. 1.2 in chapter "Bands and Bandgaps in Solids."

It is instructive to look at an enlarged detail of Fig. 13 as shown in Fig. 14d. This figure can be constructed from two parabolas of free electrons, shifted by $\frac{2\pi}{a}$ – a situation that can be thought of by inserting a lattice into the vacuum, although with vanishing lattice potential (an *empty lattice*– see ▶ Sect. 4.1 in chapter "Quantum Mechanics of Electrons in Crystals"). The electron in each reference system is described by its corresponding parabola (subfigure 14c). When interacting through a periodic perturbation potential of amplitude U_0, the crossing of both $E(k)$ parabolas is eliminated and a splitting occurs with a gap of the order of $|2\ U_0|$, as shown in subfigures b and d.

2.1 Newtonian Description of a Quasi-Free Electron

In many discussions about electron behavior in solids, a classical particle picture is used rather than the quantum-mechanical one of a wave packet; it is often more intuitive. Electrons behave like little balls, "sliding down" a potential hill and "scattering" upon collision with an atomic lattice defect. The picture is justified by using Bohr's *correspondence principle* near the bottom of the conduction band

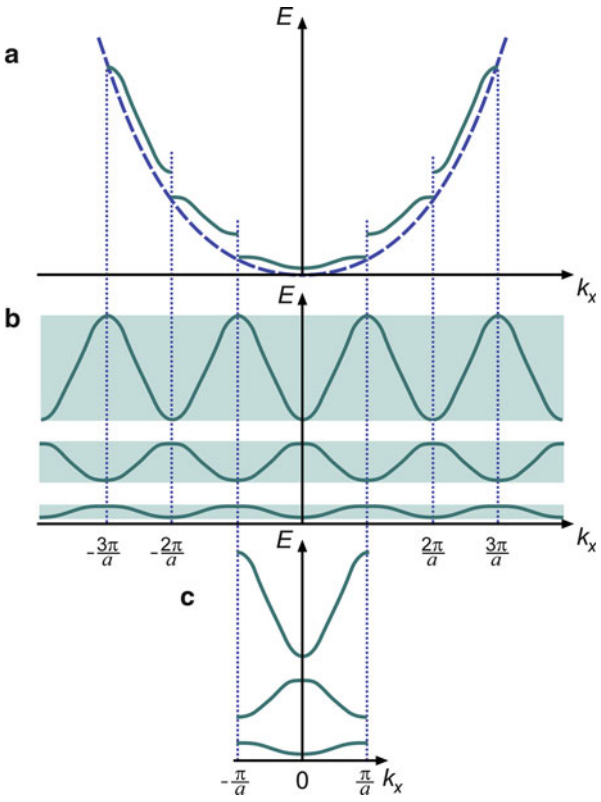

Fig. 13 Comparison between: (**a**) extended wavenumber k, (**b**) periodic, and (**c**) reduced wavenumber representations of $E(k)$

(the band in which electron conduction takes place). However, since not all of the electron behavior can be described by this model, as explained in the previous section, we can account for the modification by incorporating the information obtained from its dual nature as a wave into one of its classical parameters – its *mass*.

An electron, regarded as a classical (Newtonian) particle, has a momentum

$$p = m_0 v \quad \text{and a kinetic energy} \quad E = \frac{m_0}{2} v^2 = \frac{p^2}{2m_0}. \tag{13}$$

Relativistic effects are excluded here (i.e., $v \ll$ c is assumed): the electron mass is its rest mass m_0. The velocity of such a particle changes with time in response to an acting force $\mathcal{F}$ (*Newton's second law*):

$$\frac{dp}{dt} = m_0 \frac{dv}{dt} = \boldsymbol{\mathcal{F}}. \tag{14}$$

On the other hand, an electron in vacuum, regarded as a wave, has

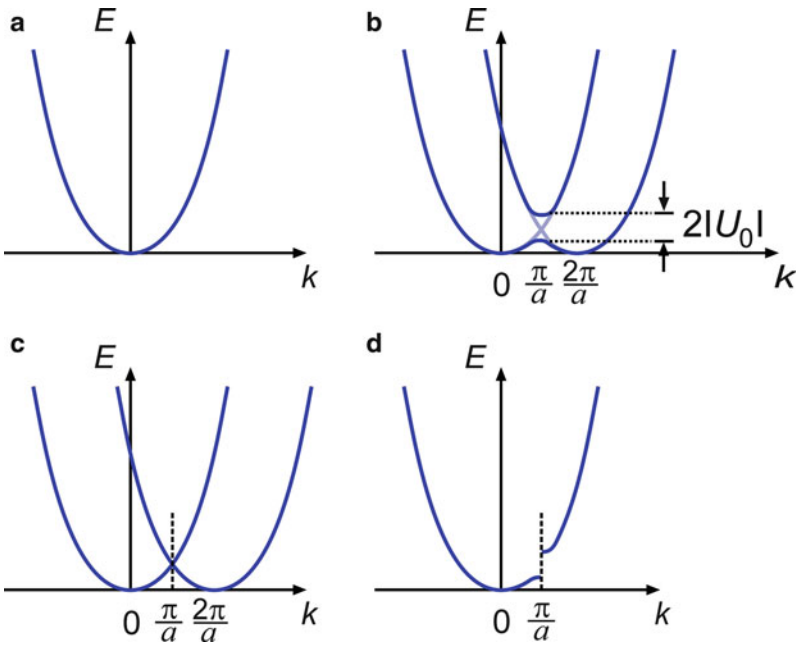

Fig. 14 (**a**) $E(k)$ for a free electron. (**b**) Splitting of $E(k)$ if a small periodic field is introduced. (**c**) Free electron in an empty lattice. (**d**) $E(k)$ of the original parabola, disturbed by the periodic-potential perturbation (compare with Fig. 13a)

$$\text{a momentum } p = \hbar k \text{ and an energy } E = \frac{p^2}{2m_0} = \frac{\hbar^2 k^2}{2m_0}. \tag{15}$$

When exposed to a force, such as that supplied by an electric field $|\mathbf{E}|$, and with $\mathcal{F} = -e|\mathbf{E}|$, its momentum increases accordingly:

$$\frac{dp}{dt} = \hbar \frac{dk}{dt} = \mathcal{F}. \tag{16}$$

When the electron is described as a *wave packet*, its velocity is the *group velocity*[6]

[6]In an infinite crystal, the electron (when not interacting with a localized defect) is not localized and is described by a simple wavefunction (i.e., having one wavelength and the same amplitude throughout the crystal). The probability of finding it is the same throughout the crystal ($\propto \psi^2$). When localized, the electron is represented by a superposition of several wavefunctions of slightly different wavelengths. The superposition of these wavefunctions is referred to as a *wave packet*. A moving electron is represented by a moving wave packet $\psi = \frac{1}{2\delta k}\int_{k-\delta k}^{k+\delta k} u(x,k)\exp(i(kx - \omega t))dk$ which quickly spreads out over time. It has its maximum at a position $\overline{x} = \frac{1}{\hbar}\frac{\partial E}{\partial k}t$, yielding for the group velocity, i.e., the velocity of the maximum of the wave packet, $v_g = \frac{\partial \overline{x}}{\partial t} = \frac{1}{\hbar}\frac{\partial E}{\partial k}$. With $E = \hbar\omega$, we obtain $v_g = \frac{\partial \omega}{\partial k}$.

$$v_g = \frac{\partial \omega}{\partial k} = \frac{1}{\hbar}\frac{\partial E}{\partial k}. \tag{17}$$

Applying Newton's law to such an electron wave packet (in a relation similar to Eq. 14),

$$m_0 \frac{dv_g}{dt} = \boldsymbol{\mathcal{F}}, \tag{18}$$

and with

$$\frac{dv_g}{dt} = \frac{1}{\hbar}\frac{d}{dt}\left(\frac{\partial E}{\partial k}\right) = \frac{1}{\hbar}\frac{\partial^2 E}{\partial k^2}\frac{dk}{dt} = \frac{1}{\hbar^2}\frac{\partial^2 E}{\partial k^2}\boldsymbol{\mathcal{F}}, \tag{19}$$

we see by comparison with Eq. 18 that the factor preceding $\boldsymbol{\mathcal{F}}$ has the dimension of an inverse mass. This factor is proportional to the curvature of $E(k)$.

2.2 The Effective Mass

If we want to retain the Newtonian behavior, we have to replace the electron mass m_0 in Eq. 18 with the *effective electron mass* when comparing Eqs. 18 and 19[7]:

$$m^* = \frac{\hbar^2}{\dfrac{\partial^2 E}{\partial k^2}}. \tag{20}$$

This effective mass contains the peculiarities of the interaction of the electron with the lattice (the superscript * distinguishes this mass from the rest mass). However, a possibly important part caused by the adiabatic approximation (see Born-Oppenheimer approximation ▶ Sect. 1.1 in chapter "Quantum Mechanics of Electrons in Crystals") is missing. The influence of this part is discussed in ▶ Sect. 1.2 in chapter "Carrier-Transport Equations" and can be described by a different effective mass – the polaron mass.

From Fig. 10, we see that the effective electron mass at the lower edge of the third band, here assumed to harbor free electrons (see ▶ Sect. 1.1 in chapter "Bands and Bandgaps in Solids"), is smaller than the rest mass of a free electron, since the curvature of $E(k)$ is larger here. At higher energies within the band, this curvature decreases, changes sign, and, at the upper edge of the band, becomes negative

[7]For the electron behavior, only *expectation values* can be given. In order to maintain Newton's second law, we continue to use $\hbar k$ (Eq. 15), which is no longer an electron momentum. It is well defined within the crystal and is referred to as *crystal momentum*. We then separate the electron properties from those of the crystal by using $\partial^2 E/\partial k^2$ to define its *effective mass*.

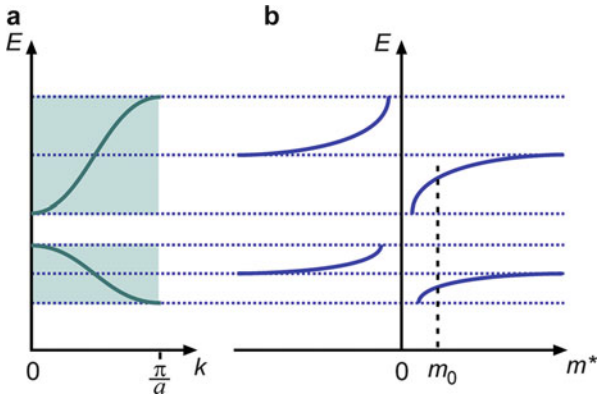

Fig. 15 (**a**) Typical $E(k)$ dependence for two simple bands, and (**b**) derived effective electron masses m^* within these permitted energy bands. Actually, one determines $m^*(k)$; this graph is turned by 90° to show its relation to the band model shown at the *left*

(as shown in Fig. 15). Consequently, the effective electron mass increases, becomes infinite near the center of an allowed band, and changes sign there. Coming from negative infinity, the effective electron mass returns to a finite but negative value which, at the top of the band, is of the same order of magnitude as at the bottom of the band (Figs. 13 and 15). This behavior is repeated in the next band, except that the sign sequence is exchanged. Here the effective mass is negative at $k = 0$; however, the effective electron mass is always positive at the bottom of any band and negative at the top. For lower bands, i.e., narrower bands, the value of the effective mass becomes larger at the band edge.

When electrons accelerate substantially above the lower edge of the band in sufficiently high fields, the de Broglie wavelength of the electron becomes smaller and comparable to the interatomic lattice spacing. Here, *interference effects* of the electron wave with the periodic lattice potential become important: Bragg reflection becomes more prevalent, while more and more frequency components of the wave packet are reflected. Therefore, further acceleration will become more difficult to achieve; in the Newtonian model, the effective mass of the electron increases until, near the center of the band, further acceleration stops. When the energy of the electron is raised above the center of the band, the electron will *decelerate* in the direction of the electric field until it reaches the top of the band, where it will come to a standstill. The electron wave has then reached a perfect diffraction condition.[8] It can be described as a *standing* wave, composed of incoming and refracted waves of exactly the same amplitude. With some caution we may describe the "recoil" of the

[8]In theory, the electron will continue to accelerate in the opposite direction to the field and lose energy, thereby descending in the band, and the above-described process will proceed in the reverse direction until the electron has reached the lower band edge, where the entire process repeats itself. This oscillating behavior is called the *Bloch oscillation*. Long before the oscillation can be completed, however, scattering interrupts the process. Whether in rare cases (e.g., in narrow mini-bands of superlattices or ultrapure semiconductors at low temperatures) such Bloch oscillations are observable, and whether they are theoretically justifiable in more advanced models (Krieger and Iafrate 1986), is controversial. In three-dimensional lattices, other bands overlap and transitions into these bands complicate the picture.

lattice as being responsible for absorbing an increasing fraction of the electron momentum when it is accelerated. The total momentum is thus still conserved, and Newton's law is fulfilled. When an electron wave impinges on a thin crystal layer in an energy range in which the crystal is partially transparent for the electron, such momentum transfer can be measured directly by changing the electron energy so that diffraction occurs and part of the electron beam is reflected.

This qualitative picture also holds for more realistic periodic potentials, although the quantitative relationship depends on many other factors. Each of the bands usually consists of several branches which often overlap one another and may show additional extrema (saddle points) in the first Brillouin zone, making the dependence of the effective mass on the electron energy more complicated. Near the band edge (for electrons), only one – perhaps degenerate – $E(k)$ branch is present in typical semiconductors, so that the above description holds rather well. This branch can be split, for example, by crystal anisotropy or electric or magnetic fields.

In summarizing the much more involved behavior of an electron in such a realistic band, we may wonder if we gained a more intuitive picture using the particle model. If we recognize, however, that the electron will mostly reside close to the bottom of the band, usually within a few kT, the model is quite helpful for an analysis of a number of basic processes. The electron will behave here like a particle with a constant effective mass; the value of this effective mass depends on the actual lattice potential, i.e., on the chemical and crystallographic nature of the material because these determine the shape of $E(k)$. In ▶ Sect. 4.5 of chapter "Carrier-Transport Equations," we present a more detailed description of the effective mass for the application of this concept to carrier transport in typical semiconductors.

3 The Proximity Approach in Organic Crystals

Organic crystals are composed of molecules as building blocks instead of atoms (▶ Sect. 1.5 in chapter "The Structure of Semiconductors"). The electronic band structure of an organic semiconductor may therefore be derived from the proximity approach (Fig. 3) by replacing energy levels of *atomic* orbitals with levels of *molecular* orbitals. A schematic of the level scheme of an isolated single molecule is shown in Fig. 16. If the molecule is electrically neutral and not a radical, it has an even number of electrons. The *highest occupied molecular orbital* of the delocalized π electrons (▶ Sect. 3.3 in chapter "Crystal Bonding") in the conjugated molecule, the so-called HOMO, refers to the electronic ground state *of the molecule*. It is occupied by 2 electrons with opposite spin and hence a singlet state with total spin $S = 0$, labeled S_0 in Fig. 16 (valence states below S_0 are not shown).

The first excited singlet state is S_1. There exists also a triplet state labeled T_1 with *parallel* spin of the electron in the HOMO state and the electron in the excited state, yielding a total spin $S = 1$; its energy is larger than that of S_0. Further excited states S_2 and T_2 may exist with an energy separation to S_0 below the ionization energy I_g, but the lifetime of an electron excited to such states is very small compared to that in the states S_1 and T_1. Excited states S_2 and T_2 as well as the vibronic states of the

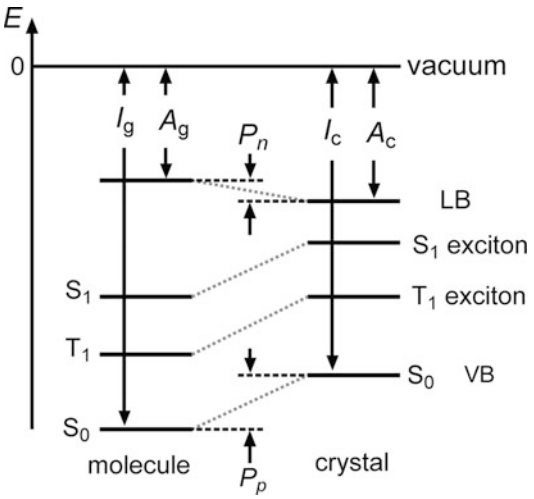

Fig. 16 Schematic of the energy levels of a single molecule (gas phase, *left*) and of a molecule crystal (*right*); I_g, A_g, I_c, and A_c denote, respectively, the ionization energies I and electron affinities A of the molecule in the gas phase and in the crystal; P_n and P_p signify the polarization energies of an electron and a hole in the molecule crystal

molecule that couple to each of the electronic states are not shown in Fig. 16 for clarity.

The molecule ground state in the gas phase is given by the ionization energy I_g. This quantity represents the energy required to remove the most weakly bound electron from the molecule and is readily accessible in experiment. Vice versa, if an additional electron is bound to the molecule to form a negatively charged molecular ion, an energy A_g, called electron affinity, is released. If the molecule is ionized in the environment of a crystal lattice, the required energy I_c is smaller than I_g, because negative and positive charges are now separated by a polarizable medium with a dielectric constant (typically about 3). I_g is reduced by a polarization energy P_p. Similarly, the electron affinity in a crystal is increased by a polarization energy P_n to a value A_c. The molecular ion states are separated by an energy gap E_g, which for $P_p = P_n \equiv P$ is given by (Karl 1974)

$$E_g = I_c - A_c = I_g - A_g - 2P = 2I_c - I_g - A_g; \tag{21}$$

see also Fig. 17. The energy gap and its position with respect to the vacuum level depend on the spatial extent of the delocalized π electrons in the molecules of the crystal; this dependence is illustrated for acenes in Fig. 17.

In an anthracene crystal the bandgap energy E_g is 4.1 eV; this energy is required to remove an electron from the HOMO level to a quasi-free state of the molecule, leaving a positive charge in the HOMO. The quasi-free state is the *lowest unoccupied molecular orbital*, the LUMO level; in analogy to inorganic semiconductors, the energy of the LUMO in organic semiconductors is referred to as *conduction band*, and that of the HOMO is called *valence band*. The S_1 state indicated in Fig. 16 lies below the LUMO level; in this state the electron is still bound to this positive charge, forming a so-called exciton (see ▶ Sect. 1.1.2 of

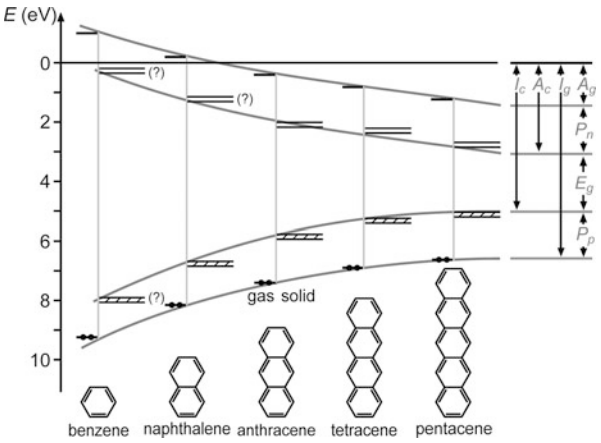

Fig. 17 Ionization energies of the highest occupied level and binding energies of the lowest unoccupied level for various oligoacenes in the gas phase (*left horizontal bars*, referring to I_g and A_g) and in the crystalline state (*right bars*, referring to I_c and A_c); after Karl (1974)

chapter "Excitons"); the excitation energy of the S_1 exciton in anthracene is 1 eV lower[9] than E_g.

The polarization energy P in organic crystals has an electronic and a vibronic component. If an electron is added to a molecule, the neighboring molecules are polarized by the negative charge in their vicinity. The characteristic response time for this *electronic polarization* is of the order of the oscillation period in an optical transition. This time is much shorter than that of a vibronic oscillation; the electronic polarization of the molecular neighborhood thus follows the movement of a quasi-free electron, thereby affecting its effective mass. This influence is not related to the effective mass of a quasi-free electron in an inorganic crystal discussed in Sect. 2. The quasi-free electron in the LUMO and its surrounding polarization cloud combined form a mobile quasiparticle referred to as (negative) *polaron*; correspondingly a positive charge in the HOMO builds a positive polaron.[10] We read from Fig. 17 that the polarization energies of the negative and positive polaron are given by

$$\begin{aligned} P_n &= A_c - A_g \\ P_p &= I_g - I_c. \end{aligned} \tag{22}$$

Both quantities are proportional to the polarizability of the organic molecules and are much larger than in conventional semiconductors. Still polarons also occur in inorganic semiconductors and are discussed in ▶ Sect. 1.2 of chapter "Carrier-Transport Equations" in the framework of transport properties.

[9]This energy difference represents the binding energy of the exciton; its value is much larger than values found in inorganic semiconductors. A large binding energy corresponds to a strong spatial localization, a typical feature of excitons in organic crystals.

[10]The polaron character of mobile carriers in organic crystal is often not explicitly considered; in analogy to the quasiparticles of inorganic semiconductors, the carriers are simply termed electrons and holes.

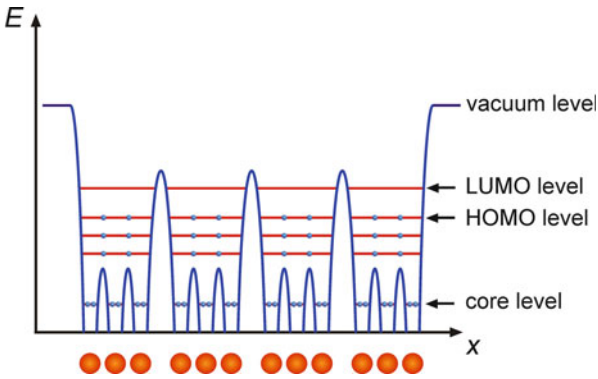

Fig. 18 Schematic of the potential energy and electron levels in a small organic crystal

The *vibronic component* of the polarization energy is related to a relaxation of the *crystal lattice* in the environment of the charged molecule. The characteristic response time is given by the period of a phonon oscillation and therefore much longer than the electronic response. A consequence of the vibronic relaxation is a decrease of the bandgap energy (in an anthracene crystal both P_n and P_p are increased by 0.15 eV; consequently E_g decreases by 0.3 eV). The energy of E_g before a lattice relaxation is called *optical bandgap* and that after relaxation *adiabatic bandgap*.

The conductivity and the carrier mobility in organic semiconductors are generally very low compared to inorganic semiconductors.[11] This holds even if the electron mobility in the LUMO level of a molecule is high. The reason is the weak intermolecular contact in the organic crystal, schematically illustrated in Fig. 18. The figure shows the potential energy and energy levels of electrons in a small crystal comprising a chain of four molecules with three atoms each. Each occupied molecular orbital is filled by two electrons with opposite spin. Above the core levels near the atomic nuclei, the schematic indicates the occupied molecular-orbital levels of electrons which are delocalized within the molecules, with the topmost HOMO state. The filled HOMO and the empty LUMO levels of each molecule are separated from those of neighboring molecules by a potential barrier. The barrier originates from the weak intermolecular van der Waals interactions, leading to a predominant localization of the HOMO and LUMO wavefunctions in each molecule. Height and thickness of this barrier decide whether – in case of small barriers, corresponding to strong intermolecular interaction – conduction and valence bands evolve from these levels or not.

If the intermolecular barrier is low, bands similar to those in inorganic semiconductors are created as illustrated in Fig. 3. Higher barriers may still allow for

[11]The mobility of electrons is defined in ▶ Sect. 2.2 in chapter "Carrier-Transport Equations" by $\mu = (q/m^*) \times \tau$, with effective mass m^*, charge q, and a mean time τ between scattering events; in organic crystals μ_{300K} is usually below 1 $cm^2/(Vs)$, often orders of magnitude smaller, compared to values of 10^3 $cm^2/(Vs)$ for inorganic semiconductors.

conductivity by phonon-assisted hopping. The criteria for the occurrence of either band conduction or hopping conduction derive from the mean time τ between scattering events of a mobile carrier and the width W of the states for carrier transport. For band conduction $\tau \gg \hbar/W$ must apply. Often a decision whether or not the criterion is met is difficult; a typical bandwidth of about 0.5 eV for oligoacene crystals yields $\tau > 10^{-15}$ s, leading to a mean free path length of the carrier that exceeds the crystal lattice constant.

4 Summary

The electronic band structure of solids is the most significant feature to understand the electronic behavior of semiconductors. General features are described by the proximity approach, which considers the effect of the immediate neighborhood in a solid and, with gradually less attention, that of more distant atoms, on the energy levels of an isolated atom. Similar results are obtained by the periodicity approach, which considers the long-range periodicity of the crystal potential. The typical band structure with alternating bands and bandgaps is characteristic for all solids, in contrast to isolated atoms which show a discrete level spectrum. Details of the band structure depend on the chemistry of the material and its atomic structure (symmetry). Deviation from a periodic structure predominantly influences the energy range near the band edges, while it has little influence near the center of the bands.

Electrons near the lower edge of a band in a periodic lattice behave akin to electrons in vacuum. The influence of the lattice is taken into account by ascribing an *effective* mass to the carriers that, for typical semiconductors, is smaller than the electron rest mass at the band edge and increases with increasing distance from the band edge. In disordered or amorphous semiconductors, the band edge is fuzzy and the electronic states become localized when extended sufficiently beyond the band edge. In organic semiconductors a large polarization affects the effective mass of carriers, accounted for in the polariton model; in the case of large intermolecular barriers hopping conduction instead of band conduction occurs.

References

Adler D (1985) Chemistry and physics of covalent amorphous semiconductors. In: Adler D, Schwartz BB, Steele MC (eds) Physical properties of amorphous materials. Plenum Press, New York, p 5–103

Agarwal SC (1995) Electronic structure of amorphous semiconductors. Bull Mater Sci 18:669

Anderson PW (1963) Concepts in solids. W. A. Benjamin, New York

Ashcroft NW, Mermin ND (1976) Solid state physics. Holt Reinhart and Winston, New York

Beeby JL, Hayes TM (1989) A calculation of the density of electronic states for amorphous semiconductors. J Non-Cryst Solids 114:253

Bloch F (1928) Über die Quantenmechanik der Elektronen in Kristallgittern. Z Phys 52:555 (On the quantum mechanics of electrons in crystal lattices, in German)

Bube RH (1992) Electrons in solids, an introductory survey, 3rd edn. Academic Press, New York
Callaway J (1976) Quantum theory of solid state. Academic Press, New York
Eberhart ME, Johnson KH, Adler D (1982) Theoretical models for the electronic structures of hydrogenated amorphous silicon. II. Three-center bonds. Phys Rev B 26:3138
Fletcher GC (1971) Electron bond theory of solids. North Holland, Amsterdam
Harrison WA (1980a) Solid state theory. Dover, New York
Harrison WA (1980b) Electronic structure and the properties of solids: the physics of chemical bonds. Freeman, San Francisco
Haug A (1972) Theoretical solid state physics. Pergamon Press, Oxford
Heine V (1980) Electronic structure from the point of view of the local atomic environment. Solid State Phys 35:1
Johnson KH, Kolari HJ, de Neufville JP, Morel DL (1980) Theoretical models for the electronic structures of hydrogenated amorphous silicon. Phys Rev B 21:643
Kaplan TA, Mahanti SD (1995) Electronic properties of solids using cluster methods. Kluwer/Plenum, New York
Karl N (1974) Organic semiconductors. Festkörperprobleme/Adv Sol State Phys 14:261
Kittel C (2007) Introduction to solid state physics, 7th edn. Wiley, New York
Krieger JB, Iafrate GJ (1986) Time evolution of Bloch electrons in a homogeneous electric field. Phys Rev B 33:5494; and (1987), Quantum transport for Bloch electrons in a spatially homogeneous electric field. Phys Rev B 35:9644
Kronig R de RL, Penney WG (1931) Quantum mechanics of electrons in crystal lattices. Proc R Soc Lond Ser A130:499
Marder MP (2010) Condensed matter physics, 2nd edn. Wiley, Hoboken
Mills RGJ, Montroll EW (1970) Quantum theory on a network. II. A solvable model which may have several bound states per node point. J Math Phys 11:2525
Ovshinsky SR, Adler D (1978) Local structure, bonding, and electric properties of covalent amorphous semiconductors. Contemp Phys 19:109
Reitz JR (1955) Methods of the one-electron theory of solids. Solid State Phys 1:1
Shinozuka Y (1999) Hybridization in electronic states and optical properties of covalent amorphous semiconductors. Mater Res Soc Symp Proc 588:309
Singh J, Shimakawa K (2003) Advances in amorphous semiconductors. CRC Press, Boca Raton
Slater JC, Johnson KH (1972) Self-consistent-field $X\alpha$ cluster method for polyatomic molecules and solids. Phys Rev B 5:844
Street RA (2005) Hydrogenated amorphous silicon. Cambridge University Press, New York
Ziman JM (1972) Principles of the theory of solids. Cambridge University Press, Cambridge